Role of the interaction matrix in mean-field spin glass models

R. Cherrier, D. S. Dean, and A. Lefèvre
IRSAMC, Laboratoire de Physique Quantique, Université Paul Sabatier, 118 route de Narbonne, 31062 Toulouse Cedex 04, France
(Received 29 November 2002; published 21 April 2003)

Mean-field models of two-spin Ising spin glasses with interaction matrices taken from ensembles that are invariant under $O(N)$ transformations are studied. A general study shows that the nature of the spin glass transition can be deduced from the eigenvalue spectrum of the interaction matrix. A simple replica approach is derived to carry out the average over the $O(N)$ disorder. The analytic results are confirmed by the extensive Monte Carlo simulations for large system sizes and by the exact enumeration for small system sizes.

DOI: 10.1103/PhysRevE.67.046112 PACS number(s): 05.50.+q, 75.10.Nr, 75.30.Fv, 75.50.Lk

I. INTRODUCTION

Mean-field models of spin glasses have been extensively studied over the last 30 years [1]. The first mean-field model to be studied thoroughly was the Sherrington-Kirkpatrick (SK) [2] model that exhibits a classical spin glass transition with a continuous transition in the Parisi overlap matrix Q_{ab} at the transition temperature T_c. The full solution to this problem requires continuous replica symmetry breaking [3], indicating an extensive number of pure states in the low temperature phase. Mean-field models with multi- or p-spin interactions exhibit discontinuous jumps in the Parisi overlap matrix Q_{ab} at the static transition temperature denoted by T_K for $p>2$ [4]. However, these systems exhibit a dynamical transition at a temperature $T_D>T_K$ indicating the onset of an extensive number of metastable states preceding the static transition. These models are of particular interest as the scenario of a dynamical transition followed by a static transition is observed in structural glasses [5,6]. For this reason the above type of behavior is often referred to as a structural glass transition. Potts-type spin glasses can also exhibit first-order phase transitions [1]. In this paper we restrict ourselves to the study of spin glasses with two-spin interactions and concentrate on the role of the interaction matrix in determining the nature of the phase transitions in the system. Mean-field spin glass type models appear in a wide range of contexts, they are of course the starting points for studying models of finite dimensional spin glasses but also arise as models of neural networks, formulations of optimization problems and simple models for protein folding.

We shall analyze a class of mean-field spin glass models with Hamiltonian

$$H=-\frac{1}{2}\sum_{ij} J_{ij}S_iS_j, \tag{1}$$

where S_i are N Ising spins. The interaction matrix J is constructed via the following procedure:

$$J=\mathcal{O}^T\Lambda\mathcal{O}, \tag{2}$$

where $\mathcal{O}$ is a random $O(N)$ matrix chosen with the Haar measure. The matrix Λ is diagonal with elements independently chosen from a distribution $\rho(\lambda)$. The support of $\rho(\lambda)$ is taken to be finite and independent of N, this ensures the existence of the thermodynamic limit. The interest of this kind of model is that one may average over the $O(N)$ disorder $\mathcal{O}$ and then examine the nature of the spin glass phase as a function of the eigenvalue distribution $\rho(\lambda)$. In particular, we shall show that the way, in which $\rho(\lambda)$ vanishes at the maximal value of its support, $\lambda_{\max}$, determines whether the glass transition is a classical spin glass transition or a structural glass transition. We show that a finite temperature classical spin glass transition occurs if the same model but with spherically constrained spins [such that $S_i\in(-\infty,\infty)$ and $\Sigma_iS_i^2=N$] exhibits a finite temperature phase transition. Where this is not the case, we study the system, using a one step replica symmetry breaking scheme, to determine the dynamical transition temperature T_D and the Kauzmann temperature T_K. Numerical simulations are carried out to confirm our analytical predictions on this class of models. We carry out both the Monte Carlo simulations and the exact enumeration calculations. The dynamical transition temperature T_D estimated from the simulations agrees well with our analytic calculations. The exact enumeration carried out on small system sizes confirms the dynamical nature of the transition occurring at T_D.

Let us briefly recall some well-studied models that fall into the class of spin glass models with interaction matrix given by the form of Eq. (2). The SK [2] model with J taken from the Gaussian ensemble $J_{ij}=J_{ji}$ and J_{ij} independent Gaussian random variables of zero mean and with $\overline{J_{ij}^2}=1/N$ can also be written in the form of Eq. (2) with the Wigner semicircle law [7] density of eigenvalues given by

$$\rho(\lambda)=\frac{(4-\lambda^2)^{1/2}}{2\pi}. \tag{3}$$

The squared interaction matrix SK (SIMSK) model studied recently in Ref. [8] has interaction matrix $J'=J^TJ$, where the interaction matrix J is taken from the Gaussian ensemble described above. Here J' is also of the form given by Eq. (2). The density of eigenvalues here is given by

$$\rho(\lambda)=\frac{(4-\lambda)^{1/2}}{2\pi\lambda^{1/2}}. \tag{4}$$

In fact the SIMSK model, at positive temperatures, is equivalent to the Hopfield model [9] with N patterns. This model

was shown [8] to have different behavior at positive and negative temperatures. In the positive temperature Hopfield model [10], the transition is a classical spin glass transition as in the SK model. However, at negative temperature the model has a structural glass transition [8]. We also note that the minority game, which is an economic model, is closely related to the negative temperature or antiferromagnetic Hopfield model and the same structural glass transition has been remarked [11]. In both the SK and SIMSK models one knows that the eigenvalues of J (the diagonal elements of Λ) are correlated [7]; however, we will see here that in the thermodynamic limit this correlation seems to be unimportant. One may also consider the more general Hopfield model with interaction matrix

$$J_{ij}=\sum_{\mu=1}^{p} x_i^\mu x_j^\mu, \tag{5}$$

where $p=\alpha N$, for α of order 1, is the number of patterns. The case where x_i^μ are Gaussian random variables of zero mean with correlation $\overline{x_i^\mu x_j^\nu}=\delta_{ij}\delta^{\mu\nu}/N$ also falls into the class of models we are considering, as an arbitrary orthogonal transformation $\mathbf{x}^\mu \to \mathcal{O}\mathbf{x}^\mu$ gives an element in the same statistical ensemble. Here the density of eigenvalues of the matrix J is [12]

$$\rho(\lambda)=\frac{[4\lambda-(\lambda+1-\alpha)^2]^{1/2}}{2\pi\lambda}+(1-\alpha)\,\delta(\lambda) \quad \text{for}$$

$$\alpha<1,\ \lambda=0,\ \text{and}\ \lambda\in[(1-\sqrt{\alpha})^2,(1+\sqrt{\alpha})^2] \tag{6}$$

$$=\frac{[4\lambda-(\lambda+1-\alpha)^2]^{1/2}}{2\pi\lambda} \quad \text{for} \quad \alpha\geqslant 1,$$

$$\lambda\in[(\sqrt{\alpha}-1)^2,(1+\sqrt{\alpha})^2]. \tag{7}$$

Hence, in the case $\alpha>1$, the density of eigenvalues is zero at the extremes of the support of $\rho(\lambda)$. In the case $\alpha\leqslant 1$, the density of eigenvalues is nonzero, and in fact diverges, at the lower band edge but stays zero at the upper band edge. We remark that the density of eigenvalues Eq. (7) when $\alpha=1$ is exactly the same density of eigenvalues as in the SIMSK model, as expected from our earlier discussion.

Another example is the random orthogonal model (ROM) studied by Marinari, Parisi, and Ritort [13], where

$$\rho(\lambda)=\alpha\,\delta(\lambda-1)+(1-\alpha)\,\delta(\lambda+1). \tag{8}$$

This model was extensively investigated in the case $\alpha=1/2$, and was shown to exhibit a structural glass transition. The case $\alpha=1/2$ is of particular interest because the high temperature series expansion in this case is equivalent to that of a frustrated mean-field model, the sine model, which has no quenched disorder. The ROM at $\alpha=1/2$ shows some rather interesting behavior, the static transition temperature T_K is extremely close to the temperature T_A where the annealed entropy vanishes. Below the static transition temperature the energy is almost constant or equivalently the specific heat is nearly zero. This implies that the ROM at $\alpha=1/2$ is *almost* a random energy model (REM) at the static level. The simplest version of the REM [14] is given by considering a system with microstates having independent energies. This situation arises by construction in the REM of Derrida where there are 2^N microstates ν of energies E_ν each chosen independently from a suitable distribution. The REM also arises when one considers the $p\to\infty$ limit of p-spin interaction mean-field spin glasses [14,15]. Another example is the case of directed polymers on Cayley trees with random bond or site disorder [16]. Although in the directed polymer problem there are correlations between paths, these correlations are weak and the resulting thermodynamics is also REM-like. In this paper we will show that this REM-like behavior is enhanced in the ROM model on increasing α above $\alpha=1/2$.

At a more technical level, the problem of averaging over the $O(N)$ disorder was solved by Marinari, Parisi, and Ritort [13] by transposing the results of Itzykson and Zuber [17] (based on generating function techniques) from the random matrix theory. For completeness we also give a simple physical (though not rigorous) rederivation of these averaging results.

II. AVERAGING OVER THE DISORDER

We consider the partition function for a model with Gaussian spins with a random interaction matrix J with density of eigenvalues λ denoted by $\rho(\lambda)$. The partition function at $\beta=1$ is given by

$$Z=\int \prod_i dS_i \exp\left(\frac{1}{2}\sum_{ij} J_{ij}S_iS_j-\frac{\mu}{2}\sum_i S_i^2\right). \tag{9}$$

The partition function may be explicitly evaluated, as in the case of the $p=2$ spherical spin glass model [18], by passing to the basis of eigenvalues of matrix J:

$$Z=\int \prod_\lambda dS_\lambda \exp\left(\frac{1}{2}\sum_\lambda \lambda S_\lambda^2-\frac{\mu}{2}\sum_\lambda S_\lambda^2\right). \tag{10}$$

The Gaussian integrals are easily performed yielding

$$Z=(2\pi)^{N/2}\prod_\lambda \frac{1}{(\mu-\lambda)^{1/2}}, \tag{11}$$

thus

$$\ln(Z)=\frac{N}{2}\ln(2\pi)-\frac{1}{2}\sum_\lambda \ln(\mu-\lambda). \tag{12}$$

Averaging over the disorder we obtain

$$g=\frac{\overline{\ln(Z)}}{N}=\frac{1}{2}\ln(2\pi)-\frac{1}{2}\int d\lambda\,\rho(\lambda)\ln(\mu-\lambda). \tag{13}$$

We will now repeat the same calculation of g by using the replica method. One replicates the system n times, where we shall consider the limit $n\to 0$:

$$Z^n = \int \prod_{i,a} dS_i^a \exp\left(\frac{1}{2} \sum_{ij} J_{ij} \sum_a S_i^a S_i^a - \frac{\mu}{2} \sum_{i,a} S_i^{a2} \right), \tag{14}$$

where $a = 1, \ldots, n$ are replica indices. In a model where the interaction matrix is chosen to give an extensive free energy, we expect that

$$\overline{\exp\left(\frac{1}{2} \sum_{ij} J_{ij} \sum_a^n S_i^a S_j^a \right)} = \exp\left(\frac{N}{2} \mathrm{Tr}\, G(Q) + \text{n.e.t.} \right), \tag{15}$$

where Tr indicates the matricial trace over the Parisi order parameter matrix $Q_{ab} = (1/N) \Sigma_i S_i^a S_i^b$, and the term n.e.t. denotes nonextensive terms. The idea of the calculation that follows is to calculate g by using the replica method and then extract G by comparing the result of this replica calculation with the result (13).

One has therefore, for a generic G,

$$\overline{Z^n} \sim \int \prod_{i,a} dS_i^a \exp\left(\frac{N}{2} \mathrm{Tr}\, G(Q) - \frac{\mu}{2} \sum_{i,a} S_i^{a2} \right). \tag{16}$$

We impose the constraint $N Q_{ab} = \Sigma_i S_i^a S_i^b$ with a Fourier representation of the δ function to obtain

$$\begin{aligned} \overline{Z^n} &\sim \int \prod_{a,b} d\Lambda_{ab} dQ_{ab} \prod_{i,n} dS_i^a \exp\left(\frac{N}{2} \mathrm{Tr}\, G(Q) + \frac{N}{2} \mathrm{Tr}\, \Lambda Q \right. \\ &\quad \left. - \frac{1}{2} \sum_{ab} \Lambda_{ab} \sum_i S_i^a S_i^b - \frac{\mu}{2} \sum_{i,a} S_i^{a2} \right) \\ &\sim \int \prod_{a,b} d\Lambda_{ab} dQ_{ab} \exp[N S^*(Q, \Lambda)], \end{aligned} \tag{17}$$

where the action $S^*(Q, \Lambda)$ over the order parameters Q and Λ is given by

$$\begin{aligned} S^*(Q, \Lambda) = \tfrac{1}{2} [&\mathrm{Tr}\, G(Q) + \mathrm{Tr}\, Q\Lambda - \mathrm{Tr} \ln(\Lambda + \mu I) \\ &+ n \ln(2\pi)]. \end{aligned} \tag{18}$$

The saddle point equations $\partial S^* / \partial \Lambda_{ab} = 0$ yield the relation $Q = (\Lambda + \mu I)^{-1}$, thus giving the result

$$\begin{aligned} \frac{\ln(\overline{Z^n})}{nN} = \frac{1}{2} \ln(2\pi) + \frac{1}{2} - \frac{1}{2n} \mathrm{extr}_Q [&\mu \mathrm{Tr}\, Q - \mathrm{Tr}\, G(Q) \\ &- \mathrm{Tr} \ln(Q)], \end{aligned} \tag{19}$$

where extr_Q indicates that the function in the square brackets is evaluated at an extremal or stationary point. For integer n this extremal value is of course the maximum; however, in the limit $n \to 0$ it is often the minimal value that should be taken. The nature of the stationary point chosen depends on the stability analysis of the Hessian matrix at that point.

We now consider what form of ansatz one should make for Q in the variational problem contained in Eq. (19). The physical nature of the problem makes it clear that the ansatz should be replica symmetric, the system minimizes its energy on condensing near maximal eigenvalues of the matrix J and there is no frustration. We make the ansatz $Q = q_0 I + qU$, where $U_{ab} = 1$ for all a, b. Making use of the fact that $U^2 = nU$, in the limit $n \to 0$, we obtain

$$\begin{aligned} g = \lim_{n \to 0} \frac{\ln(\overline{Z^n})}{nN} = \frac{1}{2} + \frac{1}{2} \ln(2\pi) - \frac{1}{2} \mathrm{extr}_{q_0, q} \Big[&\mu(q_0 + q) \\ &- G(q_0) - q G'(q_0) - \ln(q_0) - \frac{q}{q_0} \Big]. \end{aligned} \tag{20}$$

The stationarity condition with respect to q yields $G'(q_0) - \mu + 1/q_0 = 0$, which then gives

$$g = \tfrac{1}{2} + \tfrac{1}{2} \ln(2\pi) - \tfrac{1}{2} \mathrm{extr}_{q_0} [\mu q_0 - G(q_0) - \ln(q_0)]. \tag{21}$$

If one returns to the expression for the action in Eq. (19), it is easy to understand the result in Eq. (21). The term in square brackets in Eq. (19) clearly possesses an $O(n)$ invariance, which is a consequence of the $O(N)$ invariance of the original problem before the disorder average is carried out. The action (19) can therefore be written in terms of the eigenvalues of the matrix of Q_{ab}, which by comparison with Eq. (21) must correspond to the possible values of q_0. We now equate two different calculations for g, Eq. (13) and Eq. (21), to obtain

$$\min_{q_0} [\mu q_0 - G(q_0) - \ln(q_0)] = 1 + \int d\lambda \rho(\lambda) \ln(\mu - \lambda). \tag{22}$$

The function

$$f(\mu) = 1 + \int d\lambda \rho(\lambda) \ln(\mu - \lambda) \tag{23}$$

is clearly concave for $\mu > \lambda_{\max}$, where $\lambda_{\max}$ is the largest eigenvalue of the interaction matrix J. Hence, the right-hand side of Eq. (22) has the form of a Legendre transform, which can now be inverted to give the result

$$G(z) = \mathrm{extr}_\mu \left[\mu z - \int d\lambda \rho(\lambda) \ln(\mu - \lambda) \right] - \ln(z) - 1, \tag{24}$$

or explicitly

$$G(z) = z \mu(z) - \int d\lambda \rho(\lambda) \ln[\mu(z) - \lambda] - \ln(z) - 1, \tag{25}$$

where $\mu(z)$ is given by the solution to

$$z = \int \frac{\rho(\lambda) d\lambda}{\mu(z) - \lambda}. \tag{26}$$

The concavity of $f(\mu)$ furthermore assures the uniqueness of $\mu(z)$, and hence the annealed calculation (with $n = 1$ replicas) is equivalent to the quenched calculation (with $n = 0$ replicas). Hence the extremum taken in Eq. (24) should be a minimum. Consequently, we obtain the final result

$$G(z)=\min_{\mu}\left[\mu z-\int d\lambda\rho(\lambda)\ln(\mu-\lambda)\right]-\ln(z)-1. \tag{27}$$

This result can be shown to be identical to that used by Marinari, Parisi, and Ritort [13] who transposed the results of Itzykson and Zuber [17] for integrals over unitary matrices to integrals over orthogonal matrices. We recall briefly the prescription of Ref. [13] in the form adapted to the definition of the Hamiltonian used here (there is a difference of definition by a factor of 2). In the method of Ref. [13] $G(z)$ is given by

$$G(z)=\int_0^1\frac{\psi(tz)-1}{t}dt, \tag{28}$$

where

$$\psi(z)=\int d\lambda\rho(\lambda)\frac{1}{1-j(z)\lambda}, \tag{29}$$

with $j(z)$ given by the solution to the equation

$$z=j(z)\int d\lambda\rho(\lambda)\frac{1}{1-j(z)\lambda}. \tag{30}$$

Comparison of Eq. (30) with Eq. (26) shows that $\mu(z)=1/j(z)$. In addition, one sees from Eqs. (29) and (30) that $\psi(z)=z/j(z)=z\mu(z)$. When $z\ll 1$ one has the solution $\mu(z)\approx 1/z$, or $j(z)\approx z$ from Eq. (26). In both prescriptions this yields (as it should) $G(0)=0$. One also has that $\psi(0)=1$; thus differentiating Eq. (28) yields

$$G'(z)=\mu(z)-\frac{1}{z}, \tag{31}$$

which is the same equation as obtained on differentiating our result Eq. (27). The equivalence of the two averaging results is thus demonstrated. One of the advantages with the derivation of the averaging formula derived here is that it has a variational form.

Here we shall give some specific examples of $G(z)$ for some well-known models and others we will study in this paper.

The Sherrington-Kirkpatrick model. The first example to consider is the Sherrington-Kirkpatrick model, for which function G is known by simply averaging over the independent Gaussian elements of J: $G(z)=z^2/2$. We shall show how to get this result from the formalism developed above.

From Eq. (26),

$$z=\frac{1}{2\pi}\int_{-2}^{2}d\lambda\frac{\sqrt{4-\lambda^2}}{\mu(z)-\lambda}=\frac{\mu(z)-\sqrt{\mu(z)^2-4}}{2}. \tag{32}$$

Solving this gives

$$\mu(z)=z+\frac{1}{z}, \tag{33}$$

which gives $G(z)=z^2/2$ by using Eq. (31).

The Hopfield model. For all α, Eq. (26) yields

$$z=\frac{1}{2\mu}\{\mu-\alpha+1-[(\mu-\alpha+1)^2-4\mu]^{1/2}\}. \tag{34}$$

The solution to this equation turns out to be surprisingly simple and is

$$\mu=-\frac{\alpha}{1-z}+\frac{1}{z}. \tag{35}$$

Again integrating Eq. (31) gives

$$G(z)=-\alpha\ln(1-z). \tag{36}$$

The ROM. In the ROM, Eq. (26) reads

$$z=\frac{\alpha}{\mu-1}+\frac{1-\alpha}{\mu+1}. \tag{37}$$

Solving this yields

$$\mu=\frac{1\pm[1+4z(m+z)]^{1/2}}{2z}, \tag{38}$$

where $m=2\alpha-1$. The solution of μ should always be such that $\mu>\lambda_{max}$; hence we take the positive root in the above equation. The subsequent integration of Eq. (31) then gives

$$\begin{aligned}G(z)=\tfrac{1}{2}([1+4z(m+z)]^{1/2}&+m\ln\{[1+4z(m+z)]^{1/2}\\&+2z+m\}-\ln\{[1+4z(m+z)]^{1/2}+1+2mz\}\\&-m\ln(m+1)-1-\ln(2)).\end{aligned} \tag{39}$$

Setting $m=0$ yields the symmetric case $\alpha=1/2$ [13]. For this special case, the partition function may be computed directly by using the $O(N)$ invariance [19].

The semisquare law. The semisquare model is one with eigenvalues distributed uniformly between -1 and 1 and hence $\rho(\lambda)=1/2$ for $\lambda\in[-1,1]$. In this case the Eq. (26) is

$$z=\frac{1}{2}\ln\left(\frac{\mu+1}{\mu-1}\right). \tag{40}$$

This leads to

$$G(z)=\ln\left(\frac{\sinh(z)}{z}\right). \tag{41}$$

III. THE GENERAL CASE

A. Representations of the Saddle Point Action

We repeat the precedent calculation for an Ising spin Hamiltonian of form given in Eq. (1). Using the same technique as the previous section, after a little algebra, one finds

$$\frac{\ln(\overline{Z^n})}{N}=\mathrm{extr}_{Q,\Lambda}S^{**}[Q,\Lambda], \tag{42}$$

where

$$S^{**}[Q,\Lambda]=\frac{1}{2}\mathrm{Tr}\,G(\beta Q)+\frac{1}{2}\mathrm{Tr}\,Q\Lambda + \ln\left[\mathrm{Tr}_{S_a}\exp\left(-\frac{1}{2}\sum_{a,b}\Lambda_{ab}S_aS_b\right)\right]. \quad (43)$$

This is the general form used in Ref. [13]. However, as the form of G is in general rather complicated, one may use the variational representation of Eq. (27), introducing an additional order parameter matrix R to write

$$\frac{\ln(\overline{Z^n})}{N}=\mathrm{extr}_{Q,\Lambda,R}S^*[Q,\Lambda,R], \quad (44)$$

where

$$S^*[Q,\Lambda,R]=\frac{\beta}{2}\mathrm{Tr}\,QR-\frac{1}{2}\mathrm{Tr}\int d\lambda\,\rho(\lambda)\ln(R-\lambda) - \frac{1}{2}\mathrm{Tr}\ln(\beta Q)-\frac{n}{2}+\frac{1}{2}\mathrm{Tr}\,Q\Lambda + \ln\left[\mathrm{Tr}_{S_a}\exp\left(-\frac{1}{2}\sum_{a,b}\Lambda_{ab}S_aS_b\right)\right]. \quad (45)$$

The saddle point equation $\partial S^*/\partial Q=0$ yields the relation $\Lambda=Q^{-1}-\beta R$, and this leads to

$$\frac{\ln(\overline{Z^n})}{N}=\mathrm{extr}_{Q,R}S[Q,R], \quad (46)$$

where

$$S[Q,R]=-\frac{1}{2}\mathrm{Tr}\int d\lambda\,\rho(\lambda)\ln(R-\lambda)-\frac{1}{2}\mathrm{Tr}\ln(\beta Q) + \ln\left[\mathrm{Tr}_{S_a}\exp\left(\frac{1}{2}\sum_{a,b}(\beta R_{ab}-[Q]^{-1}_{ab})S_aS_b\right)\right]. \quad (47)$$

The saddle point equations for this action yield

$$Q_{cd}=\frac{\mathrm{Tr}_{S_a}S_cS_d\exp\left[\frac{1}{2}\sum_{a,b}(\beta R_{ab}-[Q]^{-1}_{ab})S_aS_b\right]}{\mathrm{Tr}_{S_a}\exp\left[\frac{1}{2}\sum_{a,b}(\beta R_{ab}-[Q]^{-1}_{ab})S_aS_b\right]}, \quad (48)$$

and

$$\beta Q=\int d\lambda\,\rho(\lambda)(R-\lambda)^{-1}. \quad (49)$$

The problem may also be formulated purely in terms of the Parisi overlap matrix Q. In this version one has

$$\frac{\ln(\overline{Z^n})}{N}=\mathrm{extr}_Q S[Q], \quad (50)$$

where

$$S[Q]=\frac{1}{2}\mathrm{Tr}\,G(\beta Q)-\frac{\beta}{2}\mathrm{Tr}\,QG'(\beta Q) + \ln\left[\mathrm{Tr}_{S_a}\exp\left(\frac{\beta}{2}\sum_{a,b}[G'(\beta Q)]_{ab}S_aS_b\right)\right]. \quad (51)$$

Here we can show that if one uses the density of eigenvalues for the SK, SIMSK, or Hopfield model in the above formula (51), the saddle point action for the corresponding model is reproduced. Any effects due to correlations between the eigenvalues presumably only show up as finite size corrections.

B. The Replica Symmetric and Annealed Cases

We start by computing the annealed free energy, which is presumably the correct free energy at sufficiently high temperatures. In the annealed case, that is, $n=1$, the free energy is given by

$$f_{ann}=-\frac{\ln(2)}{\beta}-\frac{1}{2\beta}G(\beta) \quad (52)$$

and the entropy is given by

$$s_{ann}=\ln(2)+\frac{1}{2}G(\beta)-\frac{\beta}{2}G'(\beta). \quad (53)$$

In the replica symmetric (RS) ansatz $Q_{ab}=(1-q)\delta_{ab}+q$, where δ is the Kronecker symbol, and the action reads to order n,

$$S[Q]=nS_{RS}[q]=\frac{1}{2}[G(\beta(1-q))+\beta qG'(\beta(1-q)) - \beta^2q(1-q)G''(\beta(1-q))] + \int_{-\infty}^{\infty}\frac{dz}{\sqrt{2\pi}}e^{-z^2/2}\ln\{2\cosh[\beta z\sqrt{qG''(\beta(1-q))}]\} \quad (54)$$

and the derivative of $S_{RS}[q]$ with respect to q is

$$\frac{dS_{RS}[q]}{dq}=\frac{\beta^2}{2}[G''(\beta(1-q))-\beta qG'''(\beta(1-q))]\left[q - \int_{-\infty}^{\infty}\frac{dz}{\sqrt{2\pi}}e^{-z^2/2}\tanh^2[\beta z\sqrt{qG''(\beta(1-q))}]\right]. \quad (55)$$

There are two replica symmetric saddle point equations:

$$G''(\beta(1-q))=\beta qG'''(\beta(1-q)) \quad (56)$$

and

$$q=\int_{-\infty}^{\infty}\frac{dz}{\sqrt{2\pi}}e^{-z^2/2}\tanh^2[\beta z\sqrt{qG''(\beta(1-q))}]. \quad (57)$$

The first solution is unphysical [8], and thus q is given by Eq. (57). If we look for a second-order phase transition, expanding near $q=0$, we find that a continuous nonzero solution can appear at $T_c=1/\beta_c$, where β_c is determined by

$$\beta_c^2 G''(\beta_c)=1. \quad (58)$$

This general equation was also derived in Ref. [13]. Now using Eq. (31), Eq. (58) becomes

$$\int d\lambda\,\frac{\rho(\lambda)}{(\mu_c-\lambda)^2}=\infty \quad (59)$$

and hence $\mu_c=\lambda_{\max}$, where $\lambda_{\max}$ is the largest eigenvalue of J. We thus find that T_c is given by

$$\frac{1}{T_c}=\int d\lambda\frac{\rho(\lambda)}{\lambda_{\max}-\lambda}. \quad (60)$$

It is straightforward to see that the possibility of having a finite temperature phase transition in this Ising spin model depends on the existence of a finite temperature phase transition in the corresponding spherical model. In this case the critical temperature T_c of the two transitions are the same. Equation (60) determining T_c shows that if $\rho(\lambda)/(\lambda_{max}-\lambda)$ is integrable over the support of $\rho(\lambda)$ then T_c is finite, if it is not integrable then $T_c=0$. Hence, if $\rho(\lambda)\sim(\lambda_{\max}-\lambda)^{\gamma}$ near λ_{max} then $T_c=0$, for $\gamma\leqslant 0$ but a finite temperature second-order phase transition is possible for $\gamma>0$. From Eq. (59) we also see that if $\gamma>2$ then the phase transition can be continuous but of higher than second order.

The above results can be further verified in a more general than replica symmetric context by carrying out a Landau expansion. Writing $Q_{ab}=\delta_{ab}+\omega_{ab}$, the lowest-order expansion around $\omega=0$ of Eq. (51) is

$$S[Q]=\frac{n}{2}G(\beta)+\frac{\beta^2}{2}G''(\beta)[\beta^2G''(\beta)-1]\mathrm{Tr}\,\omega^2+o(\omega^2). \quad (61)$$

The nature of the phase transition depends on the coefficient of $\mathrm{Tr}\,\omega^2$ in the expansion above. This coefficient only vanishes at $\beta^2G''(\beta)=1$, which agrees with the previous definition of T_c. If $T_c\neq 0$, then a second-order phase transition occurs at T_c, and the subsequent replica symmetry breaking is determined in terms of higher order in ω in the expansion Eq. (61). We note that the breaking of the $O(n)$ symmetry in replica space should favor replica symmetry breaking [3].

In addition if we look at the Thouless-Anderson-Palmer (TAP) equations [20] in an external field, the linear expansion in the paramagnetic phase gives the following equations for the magnetizations m_i:

$$m_i=\beta h_i+\beta\sum_{ij}J_{ij}m_j-\beta G'(\beta)m_i. \quad (62)$$

Hence, the staggered susceptibility in the direction of an eigenvalue λ is

$$\chi_\lambda=\frac{\beta}{1-\beta\lambda+\beta G'(\beta)} \quad (63)$$

$$=\frac{1}{\mu-\lambda}, \quad (64)$$

from Eq. (31). Hence, the staggered susceptibility for the maximum eigenvalue $\lambda_{\max}$ diverges at the critical temperature, as in the SK model [2].

We may now classify the phase transitions in the various models discussed here simply by examining the behavior of the density of eigenvalues $\rho(\lambda)$ at its upper band edge.

(1) SK model [Eq. (3)]: $\gamma=1/2$—second order.

(2) Hopfield $\beta>0$ [Eqs. (6) and (7)]: $\gamma=1/2$—second order.

(3) Hopfield $\beta<0$, $\alpha>1$ [Eq. (7)]: $\gamma=1/2$—second order.

(4) Hopfield $\beta<0$, $\alpha<1$ [Eq. (6)]: δ function at $\lambda_{\max}$—first order.

(5) SIMSK (Hopfield at $\alpha=1$) $\beta<0$ [Eq. (4)]: $\gamma=-1/2$—first order.

(6) ROM [Eq. (8)]: δ function at $\lambda_{\max}$—first order.

(7) Semisquare model: $\gamma=0$—first order.

C. One Step Replica Symmetry Breaking

In a variety of models such as the SK model, the Hopfield model, or the ROM, either the RS entropy or the annealed one is negative at low temperature. In this case, replica symmetry has to be broken. Indeed, the glass transition may be attributed to the existence of an extensive number of pure states. The complexity of these pure states can be computed within the following one step replica symmetry breaking (1RSB) ansatz [5,21]: Q is a block diagonal matrix, where the blocks have size $m\times m$ and $m\leqslant 1$. Inside the blocks $Q_{ab}=(1-q)\delta_{ab}+q$, then the action reduces to

$$S[q,m]=\frac{m-1}{2m}G(\beta(1-q))+\frac{1}{2m}G(\beta(1-q+qm))-\frac{\lambda}{2}(1-q+mq)+\frac{1}{m}\ln\left(\int_{-\infty}^{\infty}\frac{dz}{\sqrt{2\pi}}e^{-z^2/2}\cosh^m(\sqrt{\lambda}z)\right), \quad (65)$$

where

$$\lambda=\frac{\beta}{m}[G'(\beta(1-q+mq))-G'(\beta(1-q))]. \quad (66)$$

Expanding $S[q,m]$ around $m=1$ gives

$$S[q,m]=-\beta f_{ann}+(m-1)V(q)+o((1-m)^2). \quad (67)$$

The extremum of the effective potential $V(q)$ at $q=0$ contributes to the paramagnetic value $-\beta f_{ann}$, whereas a local

minimum at nonzero q corresponds to the entropy of pure states. The potential is easily computed,

$$V(q)=\left.\frac{\partial S[q,m]}{\partial m}\right|_{m=1} \tag{68}$$

,

$$=-\frac{1}{2}[G(\beta(1-q))-G(\beta)+\beta qG'(\beta)]+\frac{1+q}{2}\lambda$$

$$-e^{-\lambda/2}\int_{-\infty}^{\infty}\frac{dz}{\sqrt{2\pi}}e^{-z^2/2}\cosh(\sqrt{\lambda}z)\ln\cosh(\sqrt{\lambda}z), \tag{69}$$

where

$$\lambda=\beta[G'(\beta)-G'(\beta(1-q))]. \tag{70}$$

This is exactly the expression for the annealed complexity of the solutions of the TAP equations found in Ref. [20].

The dynamical transition occurs when the number of pure states becomes extensive. The dynamical transition temperature T_D and the dynamical overlap q_D are determined from the equations $V''(q_D)=V'(q_D)=0$ $(q_D\neq 0)$. The static transition occurs when the number of pure states is no longer extensive, so the static transition temperature T_K and the static overlap q_S are determined from the equations $V(q_S)=V'(q_S)=0$ $(q_S\neq 0)$.

The first derivative of the potential is

$$V'(q)=\frac{\beta^2}{2}G''(\beta(1-q))[q-\Gamma(q)], \tag{71}$$

where

$$\Gamma(q)=e^{-\lambda/2}\int_{-\infty}^{\infty}\frac{dz}{\sqrt{2\pi}}e^{-z^2/2}\tanh^2(\sqrt{\lambda}z)\cosh(\sqrt{\lambda}z) \tag{72}$$

and the second derivative is

$$V''(q)=\frac{\beta^2}{2}G''(\beta(1-q))[1-\Gamma'(q)]$$

$$-\frac{\beta^3}{2}G'''(\beta(1-q))[q-\Gamma(q)]. \tag{73}$$

After some algebra, one finds for q^* such that $V'(q^*)=0$,

$$V''(q^*)=\frac{\beta^2}{2}G''(\beta(1-q^*))\left(1-\beta^2G''(\beta(1-q^*))e^{-\lambda/2}\right.$$

$$\left.\times\int_{-\infty}^{\infty}\frac{dz}{\sqrt{2\pi}}e^{-z^2/2}\frac{1}{\cosh^3(\sqrt{\lambda}z)}\right). \tag{74}$$

The paramagnetic solution $q=0$ is always a stationary point of $V(q)$ and the second derivative of V is

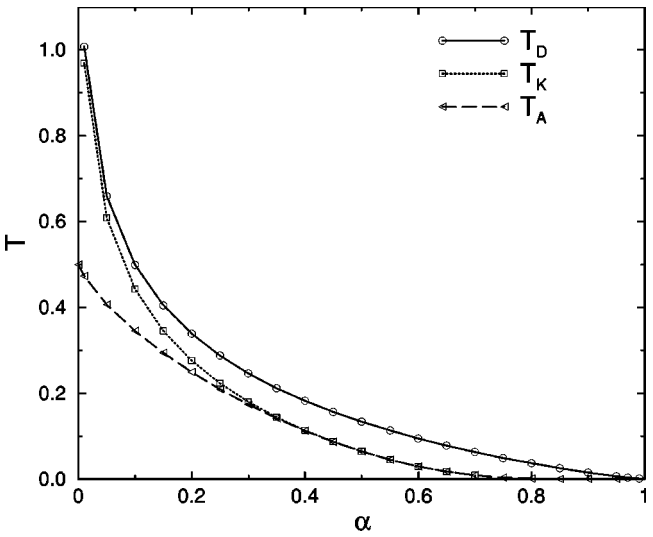

FIG. 1. Various temperatures arising in the random orthogonal model as a function of α.

$$V''(0)=\frac{\beta^2}{2}G''(\beta)[1-\beta^2G''(\beta)]. \tag{75}$$

Again, this quantity may have several possible behaviors, depending on β_c.

(1) $\beta_c=\infty$. One sees from Eq. (26) that for all temperatures $\beta^2G''(\beta)<1$, and then $V''(0)>0$. Hence, either the only local minimum of the effective potential is at $q=0$, or there is another solution appearing at $T_D>0$, where the system undergoes a dynamical transition, with a nonzero dynamical overlap q_D.

(2) $\beta_c=1/T_c<\infty$. From Eq. (26), $\beta^2G''(\beta)<1$ if $\beta<\beta_c$ and $\beta^2G''(\beta)\geqslant 1$ if $\beta\geqslant\beta_c$. Here, the stationary point $q=0$ becomes unstable at $T=T_c$, so there is no dynamical transition below T_c (one cannot exclude a dynamical transition at $T_D\neq 0$, but as expected $T_c\leqslant T_D$). We remark from Eq. (74) that if G' is convex, then there is no discontinuous dynamical transition and the system undergoes a classical spin glass transition at T_c.

This 1RSB calculation can be done for the random orthogonal model, where a discontinuous dynamical transition is expected. The dynamical and static temperatures T_D and T_K arising in the random orthogonal model as a function of α are shown in Fig. 1. Also shown is the temperature T_A at which the annealed entropy disappears. It was noted by Marinari, Parisi, and Ritort that for the ROM at $\alpha=1/2$ T_A is very close to T_K. Indeed we see that for all $\alpha\geqslant 1/2$ this is the case. This means that the statics of these models for $\alpha>1/2$ is very close to that of the REM. This analogy is further supported by the values of q in the one step solution, which are already very close to 1 at T_K.

IV. NUMERICAL SIMULATIONS

In this section we describe the numerical simulations carried out to test our theoretical results. We shall concentrate on the case of the random orthogonal model at different val-

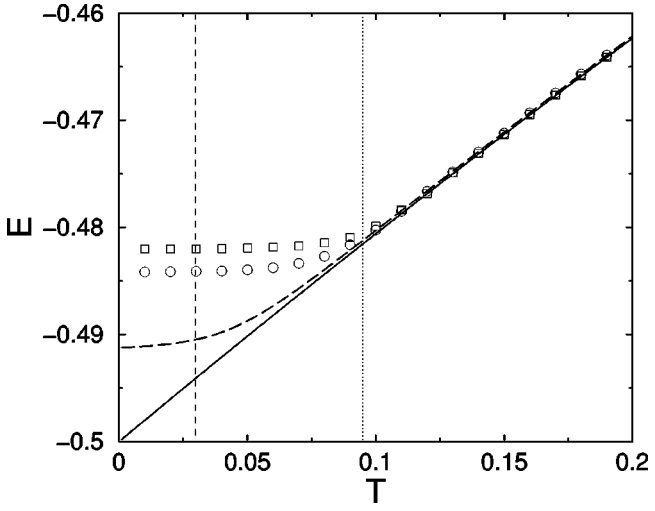

FIG. 2. Energies per spin for the ROM with $\alpha=0.6$: the Monte Carlo simulations for the systems of size $N=200$ (squares) and $N=30$ (circles), the exact enumeration for $N=30$ (long dashed line), annealed (solid line). Also shown are the calculated values of T_D (vertical dotted line) and T_K (vertical dashed line).

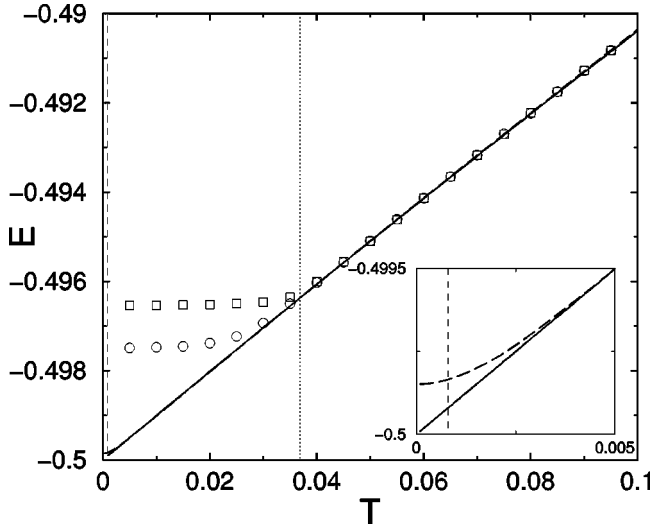

FIG. 3. Energies per spin for the ROM with $\alpha=0.8$: the Monte Carlo simulations for the systems of size $N=200$ (squares) and $N=30$ (circles), the exact enumeration for $N=30$ (long dashed line), annealed (solid line). Also shown are the calculated values of T_D (vertical dotted line) and T_K (vertical dashed line). In the inset is shown the low energy behavior of the annealed energy and the energy calculated by the exact enumeration.

ues of α and the semisquare model, which are systems exhibiting the structural glass transition.

The numerical generation of the interaction matrices J_{ij} is carried out as follows. We take a random orthonormal basis of $\mathbf{x}^{(k)}$ $1\leqslant k\leqslant N$ of $\mathbb{R}^N$ and construct J_{ij} via

$$J_{ij}=\sum_k \lambda_k x_i^{(k)} x_j^{(k)}, \tag{76}$$

where, in the case of a continuous density of eigenvalues, $\rho(\lambda)$, each λ_k is drawn independently from the distribution with probability density $\rho(\lambda)$. In the case of the ROM, in order to reduce sample to sample fluctuations, αN eigenvalues $+1$ and $N(1-\alpha)$ eigenvalues -1 are randomly assigned to each eigenvector. As mentioned above, this has the form of a Hopfield model [9] but where the patterns $\mathbf{x}^{(k)}$ are strictly orthogonal, and not simply statistically orthogonal, and where each pattern $\mathbf{x}^{(k)}$ is weighted by λ_k. The construction of a statistically $O(N)$ invariant basis $\mathbf{x}^{(k)}$ is carried out by choosing for $\mathbf{x}^{(k)}$ the (normalized) eigenvectors of the statistically $O(N)$ invariant symmetric Gaussian matrix K with $K_{ij}=\sigma_{ij}/\sqrt{N}$, each σ_{ij} being Gaussian of mean 0 and variance 1.

We have carried out two types of numerical simulations. The Monte Carlo simulations on the systems of size $N=200$ were performed, in order to validate the high temperature predictions of the theory. Below the dynamical transition temperature T_D, it is impracticable to equilibrate the system for these large system sizes; however, one may estimate the value of T_D by examining at which temperature the measured results differ from the annealed calculation. The results of our calculations are compatible with these estimations. In each of Figs. 2–4 is shown the dynamically measured energy per spin for a system of size 200. The corresponding cooling rate, the number of samples, and the number of runs are shown in Table I. The equilibration time constituted 90% of the time spent at each temperature and the measurements were made during the last 10%. Also shown in Figs. 2–4 is the calculated value of T_D (vertical dotted line) and the value of T_K (vertical dashed line). We see that for the system sizes studied here, the departure from the annealed energy and the onset of the characteristic, almost flat energy plateau, are in good agreement with the calculated value of T_D.

For the system sizes of $N=30$ spins, the energy can be calculated by exact enumeration over all the microstates. The results for the energy can be compared with those of dynami-

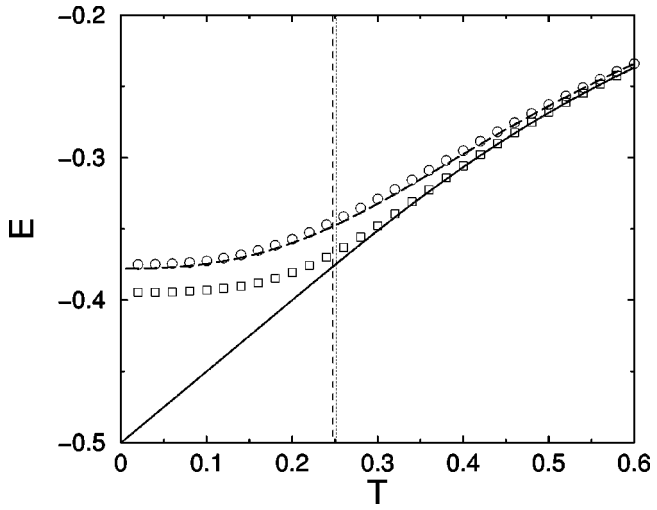

FIG. 4. Energies per spin for the semisquare model: the Monte Carlo simulations for the systems of size $N=200$ (squares) and $N=30$ (circles), the exact enumeration for $N=30$ (long dashed line), annealed (solid line). Also shown are the calculated values of T_D (vertical dotted line) and T_K (vertical dashed line).

TABLE I. Parameters used in different Monte Carlo simulations.

	Semisquare		ROM $\alpha=0.6$		ROM $\alpha=0.8$	
	$N=30$	$N=200$	$N=30$	$N=200$	$N=30$	$N=200$
Number of samples	40	40	40	40	40	40
Number of runs	200	20	200	20	200	20
Cooling rate (MCS)	5×10^5	5×10^5	10^6	10^6	2×10^6	2×10^6

cal simulations and the theoretical predictions. For the dynamical simulations on the systems of size $N=30$, the cooling rate, the number of samples, and the number of runs are also indicated in Table I. The exact enumeration averages were taken over at least 20 samples. Also shown in Figs. 2 -4 are the results of these simulations. We see that the results of the exact enumeration, even for the small system sizes used here, are in excellent agreement with the theoretical predictions. For the system with $\alpha=0.6$ (Fig. 2), we see that the plateau in the static energy is compatible with the calculated value of T_K but the Monte Carlo simulation with $N=30$ is clearly out of equilibrium at temperatures below T_D. In Fig. 3 for $\alpha=0.8$ the theoretical prediction is that $T_K \ll T_D$. We see that the exact enumeration result is in perfect agreement with the annealed energy down to energies around T_K (shown enlarged in the figure inset). The Monte Carlo results for the systems of size $N=30$ are, however, still clearly out of equilibrium. In Fig. 4 are shown the results for the semisquare model. We see that the dynamics and the Kauzmann temperatures are very close; however, here the results of the Monte Carlo simulations and the exact enumeration for the systems of size $N=30$ are much closer, the dynamically measured energies are, however, still slightly lower than the static ones measured by exact enumeration.

V. CONCLUSIONS

In this paper we have examined the statics of a class of fully connected generalized random orthogonal models. We have shown how the average over the $O(N)$ disorder can be carried out, using a simple replica method recovering the results of the random matrix theory. This method has the useful property of giving a variational form for the result. Depending on the behavior of the density of eigenvalues at the band edges, we have seen that one either obtains a classical spin glass transition or a structural glass transition. Our results suggest that in the thermodynamic limit only the density of eigenvalues is important for the statics of these models. This classification should be useful in a wide range of models. It was noted that the ROM with a bimodal distribution of eigenvalues behaves like a random energy model for large values of α, in agreement with previous studies where it was shown already to have very close to REM-like behavior at $\alpha=1/2$.

We have carried out numerical simulations on the generalized form of the original ROM model, which support our analytical calculations. Simulating small system sizes via the Monte Carlo dynamics and by the exact enumeration confirms the dynamical nature of the transition occurring at T_D. Further questions arising form this study will be interesting to address. One can look at the number of metastable states in such systems to better understand the geometric reasons leading to the glassy behavior [22]. Also the fact that even small system sizes stay out of equilibrium on numerically accessible time scales and the fact that they can be studied by exact enumeration means that one may study finite size effects and hence activated processes on the dynamical transition as proposed in Ref. [23]. The formulation of the saddle point action in Eq. (47) also allows one to study the decomposition of the Parisi overlap matrix Q on the basis of eigenvectors of the problem, which may give a more geometric picture of the nature of the glassy phase of these models.

[1] K. Binder and A.P. Young, Rev. Mod. Phys. **58**, 801 (1986); M. Mézard, G. Parisi, and M.A. Virasoro, *Spin Glass Theory and Beyond* (World Scientific, Singapore, 1987); K.H. Fischer and J.A. Hertz, *Spin Glasses* (Cambridge University Press, Cambridge, 1991); V. Dotsenko, *Introduction to the Replica Theory of Disordered Statistical Systems* (Cambridge University Press, Cambridge, 2000).

[2] D. Sherrington and S. Kirkpatrick, Phys. Rev. Lett. **35**, 1792 (1975); Phys. Rev. B **17**, 4384 (1978)

[3] G. Parisi, Phys. Rev. Lett. **43**, 1754 (1979); J. Phys. A **13**, 1101 (1980).

[4] A. Crisanti and H.J. Sommers, Z. Phys. B: Condens. Matter **87**, 341 (1992).

[5] T.R. Kirkpatrick and P.G. Wolynes, Phys. Rev. B **36**, 8552 (1987).

[6] T.R. Kirkpatrick, D. Thirumalai, and P.G. Wolynes, Phys. Rev. A **40**, 1045 (1989).

[7] M.L. Mehta, *Random Matrices and the Statistical Theory of Energy Levels* (Academic, New York, 1967).

[8] D.S. Dean and F. Ritort, Phys. Rev. B **65**, 224209 (2002).

[9] J.J. Hopfield, Proc. Natl. Acad. Sci. U.S.A. **79**, 2554 (1982).

[10] D.J. Amit, H. Gutfreund, and H. Sompolinsky, Phys. Rev. A **32**, 1007 (1985); Phys. Rev. Lett. **55**, 1530 (1985).

[11] A. De Martino and M. Marsili, J. Phys. A **34**, 2525 (2001).

[12] A. Crisanti and H. Sompolinsky, Phys. Rev. A **36**, 4922 (1987).

[13] E. Marinari, G. Parisi, and F. Ritort, J. Phys. A **27**, 7647 (1994).

[14] B. Derrida, Phys. Rev. B **24**, 2613 (1981).

[15] D.J. Gross and M. Mezard, Nucl. Phys. B **240**, 431 (1984).

[16] B. Derrida and H. Spohn, J. Stat. Phys. **51**, 817 (1988).

[17] C. Itzykson and J.B. Zuber, J. Math. Phys. **21**, 411 (1980).
[18] J.M. Kosterlitz, D.J. Thouless, and R.C. Jones, Phys. Rev. Lett. **36**, 1217 (1976).
[19] E. Brezin and D.J. Gross, Phys. Lett. **97B**, 120 (1980).
[20] M. Potters and G. Parisi, J. Phys. A **28**, 5267 (1995).
[21] R. Monasson, Phys. Rev. Lett. **75**, 2847 (1995).
[22] R. Cherrier, D.S. Dean, and A. Lefèvre (unpublished).
[23] A. Crisanti and F. Ritort, Europhys. Lett. **52**, 640 (2000).